Available online at www.sciencedirect.com
SCIENCE DIRECT
Journal of Controlled Release 102 (2005) 583–594
journal of controlled release
www.elsevier.com/locate/jconrel

Cationic charge-dependent hepatic delivery of amidated serum albumin

Shen-Feng Ma[a], Makiya Nishikawa[b], Hidemasa Katsumi[a], Fumiyoshi Yamashita[a], Mitsuru Hashida[a,*]

[a]*Department of Drug Delivery Research, Graduate School of Pharmaceutical Sciences, Kyoto University, Sakyo-ku, Kyoto 606-8501, Japan*
[b]*Department of Biopharmaceutics and Drug Metabolism, Graduate School of Pharmaceutical Sciences, Kyoto University, Sakyo-ku, Kyoto 606-8501, Japan*

Received 8 June 2004; accepted 1 November 2004
Available online 10 December 2004

Abstract

To obtain a quantitative correlation between the physicochemical properties of amidated bovine serum albumin (BSA) and their tissue distribution characteristics for the development of targeted delivery of proteins, BSA was amidated with hexamethylenediamine (HMD) or ethylenediamine (ED) to obtain cationized BSAs. Their structural changes were examined by spectroscopic and electrophoretic techniques then their tissue distribution was studied in mice. Circular dichroism (CD) and fluorescence measurements showed that spectroscopic changes occurred as the number of free NH_2 groups increased. Capillary electrophoresis revealed a linear relationship between the mobility and the increased number of free NH_2 groups. ^{111}In-cationized BSAs were rapidly taken up by liver, but HMD-BSA showed a faster uptake than ED-BSA with a similar number of free NH_2 groups, suggesting that the diamine reagent with a longer carboxyl side chain results in more efficient hepatic targeting. The hepatic uptake clearance (CL_{liver}) of both derivatives increased significantly with a decrease in electrophoretic mobility (μ_{ep}) towards the anode and reached a plateau at low electrophoretic mobility. The electrophoretic mobility is an appropriate indicator of the degree of amidation, which was closely correlated with the hepatic uptake clearance. The correlation between the mobility and the clearance shows that a low degree of amidation is sufficient for efficient hepatic targeting of proteins.

Keywords: Bovine serum albumin; Amidation; Structural changes; Tissue distribution; Pharmacokinetics

Abbreviations: BSA, bovine serum albumin; HMD, hexamethylenediamine; ED, ethylenediamine; CD, circular dichroism; DTPA, diethylenetriaminepentaacetic acid; TNBS, trinitrobenzene sulfonic acid; bis-ANS, 4,4′ -dianilino-1,1′ -binaphthyl-5,5′ -disulfonic acid; EDAC, 1-ethyl-3-[3-(dimethylamino)propyl]carbodiimide hydorochloride; CL_{liver}, hepatic clearance; μ_{ep}, electrophoretic mobility; Trp, tryptophan; Tyr, tyrosin.

* Corresponding author. Tel.: +81 75 753 4545; fax: +81 75 753 9260.
E-mail address: hashidam@pharm.kyoto-u.ac.jp (M. Hashida).

0168-3659/$ - see front matter © 2004 Elsevier B.V. All rights reserved.
doi:10.1016/j.jconrel.2004.11.006

1. Introduction

For effective drug therapy, it is necessary to deliver the therapeutic agents selectively to their target sites, since most drugs are associated with both beneficial and adverse effects. Among the various strategies for site-specific drug delivery, macromolecular carriers such as proteins and synthetic polymers are becoming widely used because of the diversity of their physicochemical and biological properties and functions [1–3]. As a method for site-specific drug delivery, chemical modification of protein carriers is an attractive strategy for the optimization of drug therapy as far as efficacy and safety are concerned.

In previous studies, we explored the tissue distribution characteristics of proteins and their derivatives in relation to their physicochemical and biological properties by examining the pharmacokinetic clearance and constructed a strategy for the rational design of targeting systems [4,5]. Based on the relationships obtained, targeted delivery systems for proteins have been developed using chemical modifications such as galactosylation, mannosylation or succinylation [6–9]. Biologically active proteins such as superoxide dismutase and catalase have been successfully targeted to liver nonparenchymal cells by succinylation or mannosylation [10,11]. During these investigations, it was found that the molecular weight and electric charge of the protein derivatives play critical roles in the tissue distribution, including the hepatic uptake, a very important distribution-determining process.

Cationization is another approach that can be used for targeted drug delivery. The cell surface membrane is negatively charged, so this charged surface provides sites of interaction for cationic macromolecules. Thus far, cationic delivery systems have been used for the delivery of drugs, proteins and genes to various tissues including the liver, brain and kidney [12]. The liver plays a significant role in the overall clearance of cationic macromolecules from the circulation because of its unique capillary architecture, and the hepatic targeting of a cationic macromolecular conjugate of mitomycin C [13] and superoxide dismutase [11] with dextran derivatives has been reported. Recently, this cationic charge-mediated delivery has been extensively studied in the field of nonviral gene delivery [14].

In spite of these promising characteristics, there are no systematic studies of the application of cationization techniques to the targeted delivery of proteins to the liver. In fact, the effects of cationization on protein conformation such as dimensional structure, fluorescent and electric properties have hardly been examined at all. In this study, therefore, the relationship between the physicochemical characteristics of macromolecules and their tissue distribution was systematically studied using bovine serum albumin (BSA, molecular weight 67 kDa) as a model protein. Two amidation reagents, ethylenediamine (ED) and hexamethylenediamine (HMD), were used for the cationization of BSA, and derivatives with different degrees of modification were synthesized. We examined the structural properties spectroscopically and electrophoretically as well as the tissue distribution characteristics of these cationized BSAs. Pharmacokinetic analyses were performed to obtain quantitative relationships between the various factors.

2. Materials and methods

2.1. Materials and animals

BSA, 1-ethyl-3-[3-(dimethylamino)propyl]carbodiimide hydorochloride (EDAC), HMD and 4,4′-dianilino-1,1′-binaphthyl-5,5′-disulfonic acid (bis-ANS) were purchased from Sigma (St. Louis, MO). BSA was defatted according to the reported method [15] before use. Diethylenetriaminepentaacetic acid (DTPA) anhydride was obtained from Dojindo Laboratory (Kumamoto, Japan). ^{111}Indium chloride ([^{111}In]$InCl_3$) was kindly supplied from Nihon Medi-Physics (Takarazuka, Japan). ED was obtained from Wako (Osaka, Japan). All other chemicals were of analytical grade.

Male ddY mice (24–26 g) were purchased from the Shizuoka Agricultural Cooperative Association for Laboratory Animals (Shizuoka, Japan). Animals were maintained under conventional housing conditions. All animal experiments were conducted in accordance with the principles and procedures outlined in the National Institute of Health Guide for the Care and Use of Laboratory Animals. The protocols for animal experiments were approved by the Animal Experi-

mentation Committee of Graduate School of Pharmaceutical Sciences of Kyoto University.

2.2. Synthesis of cationized BSAs

Derivatives of BSA with HMD (HMD-BSA) were synthesized by covalent attachment of HMD to BSA [16]. Coupling reactions of BSA with ED (ED-BSA) were performed as described previously [17]. Native and cationized BSAs were subjected to SDS-PAGE analysis, and all were found to give one band (data not shown). The number of increased free amino groups in each derivative was determined by the trinitrobenzene sulfonic acid (TNBS) method [18].

2.3. Radiolabeling of cationized BSAs and tissue distribution experiments

BSA derivatives were radiolabeled with ^{111}In using the bifunctional chelating regent DTPA anhydride according to the method of Hnatowich et al. [19], which has been described in a previous paper [8]. Mice received into the tail vein injections of ^{111}In-labelled cationized BSA at a dose of 1 mg/kg in saline and housed in metabolic cages to allow the collection of urine. At appropriate intervals after injection, blood was collected from the vena cava under ether anesthesia and plasma was obtained by centrifugation. The liver, kidney, spleen, lung, heart and muscle were excised, rinsed with saline and weighed. The radioactivity of each sample was measured in a well-type NaI scintillation counter (ARC-500, Aloka, Tokyo). Radioactivity originating from the plasma in each tissue sample was corrected using the distribution data of ^{111}In-BSA at 10 min after intravenous injection, assuming that ^{111}In-BSA was not taken up by tissues during this 10-min period.

2.4. Pharmacokinetic analysis

The plasma ^{111}In radioactivity concentrations were normalized with respect to the percentage of the dose per milliliter and analyzed using the nonlinear least-square program MULTI [20]. The tissue distribution was evaluated using the liver uptake clearance (CL_{liver}) as described previously [7,8].

2.5. Circular dichroism (CD) measurements

CD spectra were recorded using a JASCO-820 type spectropolarimeter (JASCO, Tokyo, Japan) at 25 °C. For calculation of the mean residue ellipticity [θ], the molecular mass of the BSA derivatives was assumed to be 67 kDa. Far-UV (wavelength 200–250 nm) and near-UV (wavelength 250–350 nm) CD spectra were recorded at protein concentrations of 5 and 15 μM, respectively, in 67 mM sodium phosphate buffer (pH 7.4) [21].

2.6. Fluorescence measurements

Steady-state fluorescence measurements were performed using a Shimadzu RF-540 spectrofluorophotometer (Shimadzu, Kyoto, Japan) with 1-cm quartz cells, thermostatically controlled devices and 5-nm excitation and emission bandwidths at 25 °C. A fluorescence excitation wavelength of 295 or 280 nm was employed. The protein concentration was 2 μM in 67 mM sodium phosphate buffer (pH 7.4) [22].

2.7. Effective hydrophobicity

The effective hydrophobicity of cationized BSAs was estimated as reported previously [22] with slight modifications. In brief, each cationized BSA sample was dissolved in 67 mM sodium phosphate buffer (pH 7.4) to give a final concentration of 1 μM. To this solution was added bis-ANS (1 μM) at 25 °C and the fluorescence spectra excited at 394 nm were recorded on a Shimadzu RF-540 spectrofluorophotometer using a 1-cm quartz cell, thermostatic devices and 5-nm excitation and emission bandwidths.

2.8. Capillary electrophoresis

BSA derivatives (15 μM) were dissolved in 67 mM sodium phosphate buffer (pH 3.0), which was used as a background electrolyte. A CAPI-3000 (Otsuka Electronics, Osaka, Japan) capillary electrophoresis system was equipped with a bare fused silica capillary (total length 42 cm, effective length 30 cm, inner diameter 75 μm; GL Science, Tokyo, Japan). Hexadimethrin bromide solution (5%) was delivered through the capillary before use every day.

Table 1
Number of increased free amino groups in cationized BSAs

Compound	Modifier	Number of increased free $-NH_2$ (mol/mol)
BSA		0(60)
HMD-BSA	HMD	
$HMD_{3.0}$-BSA		3.0
$HMD_{3.9}$-BSA		3.9
$HMD_{5.7}$-BSA		5.7
$HMD_{12.4}$-BSA		12.4
$HMD_{15.4}$-BSA		15.4
$HMD_{19.0}$-BSA		19.0
$HMD_{22.5}$-BSA		22.5
$HMD_{24.6}$-BSA		24.6
ED-BSA	ED	
$ED_{3.7}$-BSA		3.7
$ED_{8.4}$-BSA		8.4
$ED_{15.8}$-BSA		15.8
$ED_{21.5}$-BSA		21.5
$ED_{31.4}$-BSA		31.4
$ED_{44.2}$-BSA		44.2
$ED_{45.0}$-BSA		45.0
$ED_{49.4}$-BSA		49.4
$ED_{52.5}$-BSA		52.5
$ED_{56.7}$-BSA		56.7

The number of free amino groups was measured by the TNBS method. The number in parentheses for BSA is the number of amino groups before amidation.

A negative voltage (−10 kV) was applied to perform the electrophoresis. The electropherograms were obtained by measurement of the UV adsorption intensity at 280 nm.

3. Results

3.1. Synthesis of cationized BSAs

The carboxyl groups of BSA were amidated with HMD and ED, respectively. The modification reagents and the degree of modification of cationized BSAs are summarized in Table 1. The increase in the number of free amino groups was 3.0, 3.9, 5.7, 12.4, 15.4, 19.0, 22.5 and 24.6 for HMD-BSAs and 3.7, 8.4, 15.8, 21.5, 31.4, 44.2, 45.0, 49.4, 52.5 and 56.7 for ED-BSAs, respectively.

3.2. Structural properties of native and cationized BSAs

3.2.1. Spectroscopic properties

Fig. 1A and B shows the far-UV and near-UV CD spectra, respectively. In the far-UV region, the characteristics of $HMD_{3.0}$-BSA, $HMD_{5.7}$-BSA, $ED_{3.7}$-BSA and $ED_{8.4}$-BSA were similar to that of BSA. In the case of $HMD_{15.4}$-BSA and $ED_{15.8}$-BSA, the θ_{obs} values were higher than BSA, indicating some loss of the α-helix structure. $HMD_{24.6}$-BSA and $ED_{21.5}$-BSA showed a further increase in θ_{obs} values compared with BSA (Fig. 1A). In the near-UV region, $HMD_{3.0}$-BSA, $HMD_{5.7}$-BSA, $ED_{3.7}$-BSA and $ED_{8.4}$-BSA had similar CD spectra to BSA. Highly cationized BSAs showed some changes in their tertiary structure, indicating that denatured

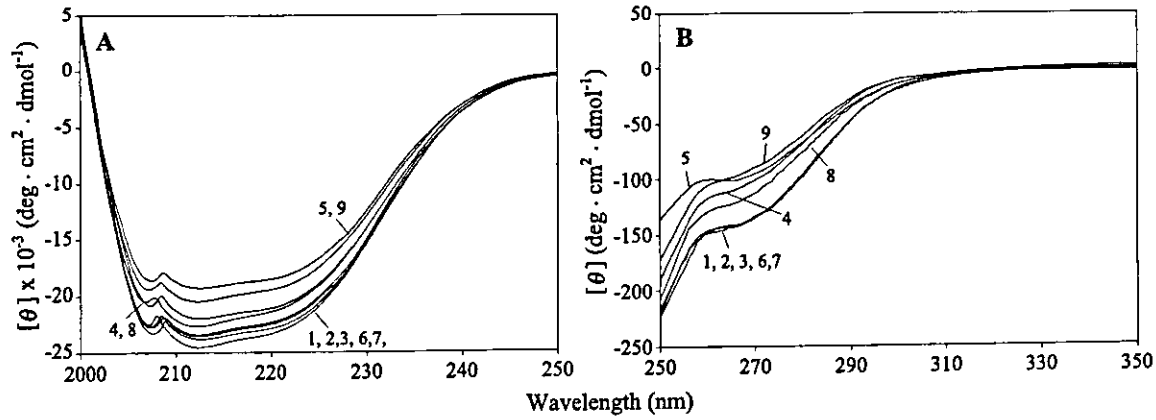

Fig. 1. Far-UV (A) and near-UV (B) CD spectra of native and cationized BSAs. (1) BSA, (2) $HMD_{3.0}$-BSA, (3) $HMD_{5.7}$-BSA, (4) $HMD_{15.4}$-BSA, (5) $HMD_{24.6}$-BSA, (6) $ED_{3.7}$-BSA, (7) $ED_{8.4}$-BSA, (8) $ED_{15.8}$-BSA, (9) $ED_{21.5}$-BSA. The protein concentration was 5 (A) and 15 μM (B) in 67 mM sodium phosphate buffer (pH 7.4), 25 °C.

changes had occurred during the chemical modification (Fig. 1B).

The effects of cationization on the intrinsic fluorescence of BSA are shown in Fig. 2A and B. In Fig. 2A, the fluorescence, which mainly is due to the excitation of tyrosine residue (Tyr) and tryptophan residue (Trp), was affected significantly by cationization in both cases of ED- and HMD-modification. The fluorescence at λ_{max} decreased from 51.4% to 27.8%, 23.2%, 20.6%, 12.8%, 20.2%, 16.7%, 12.0% and 10.7% in $HMD_{3.0}$-BSA, $HMD_{5.7}$-BSA, $HMD_{15.4}$-BSA, $HMD_{24.6}$-BSA, $ED_{3.7}$-BSA, $ED_{8.4}$-BSA, $ED_{15.8}$-BSA and $ED_{21.5}$-BSA, respectively. The λ_{max} values were blue-shifted from 343 to 339 nm in HMD–BSAs, whereas they were scarcely affected in ED-BSAs. The Trp emission spectra were obtained after excitation at 295 nm (Fig. 2B). The cationized BSAs had much lower fluorescence intensities at λ_{max}, 13.5%, 12.4%, 9.9%, 6.2%, 11.6%, 9.9%, 8.4% and 7.8% in $HMD_{3.0}$-BSA, $HMD_{5.7}$-BSA, $HMD_{15.4}$-BSA, $HMD_{24.6}$-BSA, $ED_{3.7}$-BSA, $ED_{8.4}$-BSA, $ED_{15.8}$-BSA and $ED_{21.5}$-BSA, respectively, compared with BSA (24.0%). The λ_{max} values in ED-BSAs were the same as that observed in BSA (346 nm) and they were blue-shifted to 341 nm in HMD-BSAs. These findings suggest that conformational changes in BSA take place in the vicinity of the Trp and Tyr residues during cationization as reported in the literature [23]. In addition, the effective hydrophobicity of cationized BSAs also increased with the increasing number of free amino groups (data not shown).

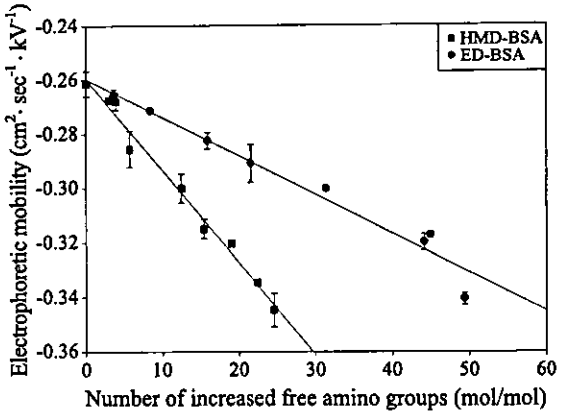

Fig. 3. Electrophoretic mobility of native and cationized BSAs as a function of the free amino groups increased per protein. HMD-BSA (■) and ED-BSA (●). The protein concentration was 15 μM in 67 mM sodium phosphate buffer (pH 3.0) at room temperature. Results are expressed as the mean±S.D. of three to four determinations.

3.2.2. Electrophoretic properties

The electrophoretic mobility (μ_{ep}) towards the anode of BSA and cationized BSAs was plotted against the increased number of free amino groups (Fig. 3). The μ_{ep} value linearly decreased as the free amino groups increased in both HMD-BSA and ED-BSA, but with different slopes of −0.0034 and −0.0015, respectively.

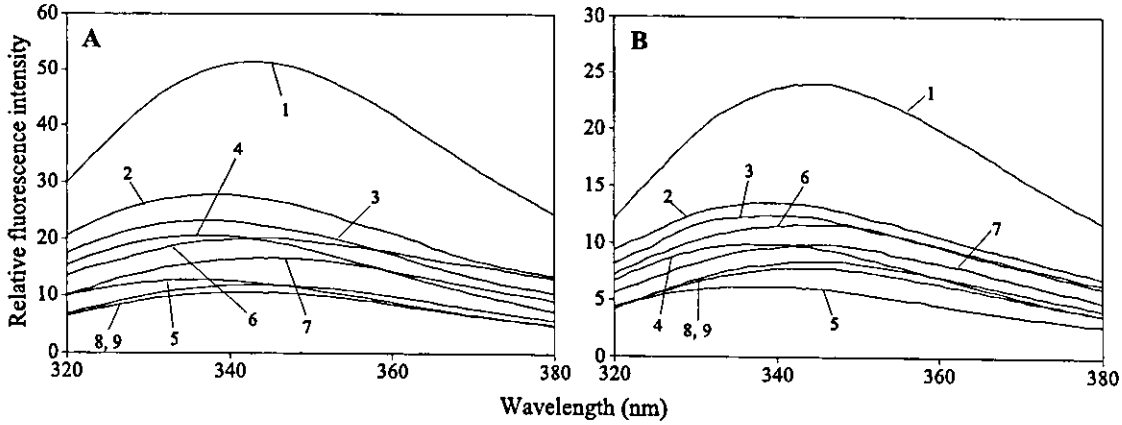

Fig. 2. Intrinsic fluorescence spectra of native and cationized BSAs excited at 280 (A) and 295 nm (B). (1) BSA, (2) $HMD_{3.0}$-BSA, (3) $HMD_{5.7}$-BSA, (4) $HMD_{15.4}$-BSA, (5) $HMD_{24.6}$-BSA, (6) $ED_{3.7}$-BSA, (7) $ED_{8.4}$-BSA, (8) $ED_{15.8}$-BSA, (9) $ED_{21.5}$-BSA. The protein concentration was 2 μM in 67 mM sodium phosphate buffer (pH 7.4), 25 °C.

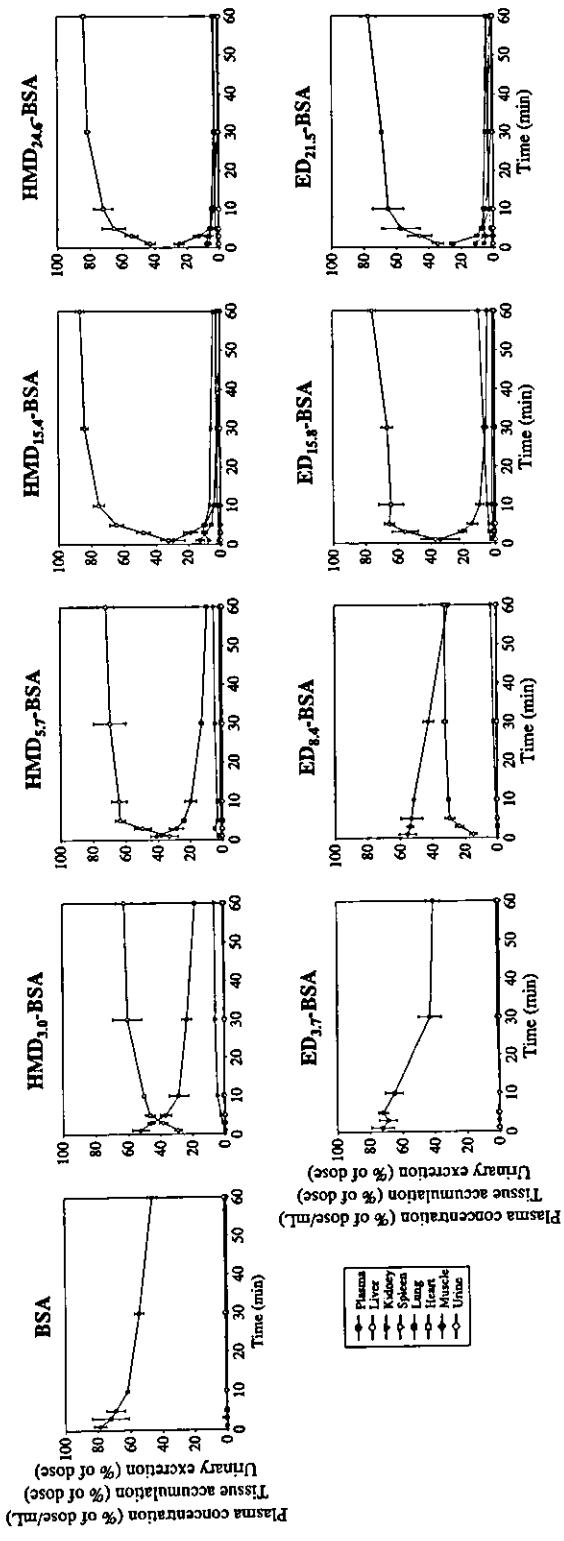

Fig. 4. Plasma concentration, tissue accumulation and urinary excretion of ^{111}In-labelled native and cationized BSAs after intravenous injection into mice at a dose of 1 mg/kg. Results are expressed as the mean±S.D. of three mice.

3.3. Tissue distribution of ^{111}In-labelled cationized BSAs

Fig. 4 shows the time-courses of the plasma concentration, tissue accumulation and urinary excretion of ^{111}In-labelled HMD-BSA and ED-BSA with different degrees of modification. These cationized BSAs showed distinct tissue distribution profiles depending on the number of increased free amino groups. Although ^{111}In-$ED_{3.7}$-BSA showed a slightly faster disappearance from blood than ^{111}In-BSA, it also remained in the blood circulation for a long period of time. The increase in the number of free amino groups of ED-BSA resulted in fast elimination from the circulation as well as an increased and more rapid hepatic uptake. Similar profiles were obtained for $HMD_{5.7}$-BSA, $HMD_{15.4}$-BSA, $HMD_{24.6}$-BSA, $ED_{15.8}$-BSA and $ED_{21.5}$-BSA. In addition, HMD-BSA showed a faster rate of liver accumulation and blood elimination than ED-BSA when these derivatives with a similar number of increased free amino groups were compared.

3.4. Quantitative analysis of spectroscopic properties of cationized BSAs

The relative fluorescence intensity at λ_{max} of HMD-BSA and ED-BSA calculated from Fig. 2, decreased differently with the number of increased free amino groups (Fig. 5A and B). When HMD-BSA and ED-BSA were compared in cases where there were a similar number of increased free amino groups, the ED-BSA derivatives showed a more rapid decrease in the relative fluorescence intensity at λ_{max} both excited at 280 and 295 nm than the HMD-BSA derivatives.

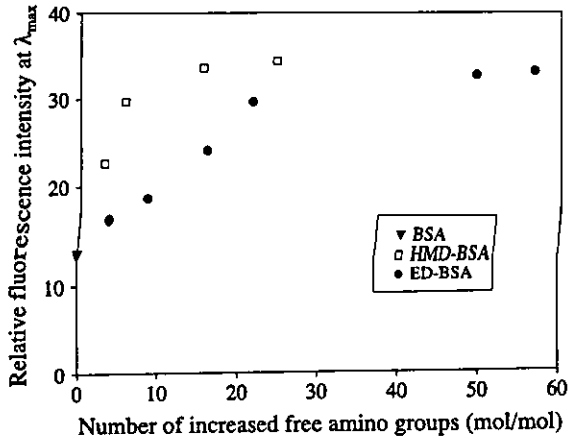

Fig. 6. Effective hydrophobicity of native and cationized BSAs as a function of the number of increased free amino groups. The concentration of protein and bis-ANS was 1 μM. BSA (▼), HMD-BSA (□), ED-BSA (●).

3.5. Quantitative analysis of effective hydrophobicity of cationized BSAs

Measurement of the exposure of the hydrophobic area of cationized BSAs using bis-ANS also showed a difference between HMD-BSA and ED-BSA (Fig. 6); the HMD-BSA derivatives exhibited a larger increase

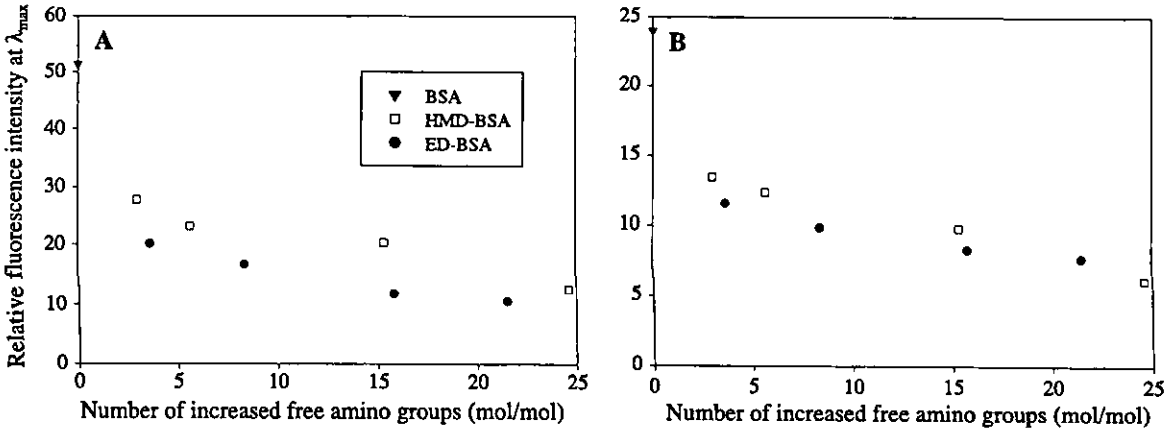

Fig. 5. Relative fluorescence intensity at λ_{max} of native and cationized BSAs as a function of the number of increased free amino groups excited at 280 (A) and 295 nm (B). The data used in this figure were calculated from Table 1 and Fig. 2. BSA (▼), HMD-BSA (□), ED-BSA (●).

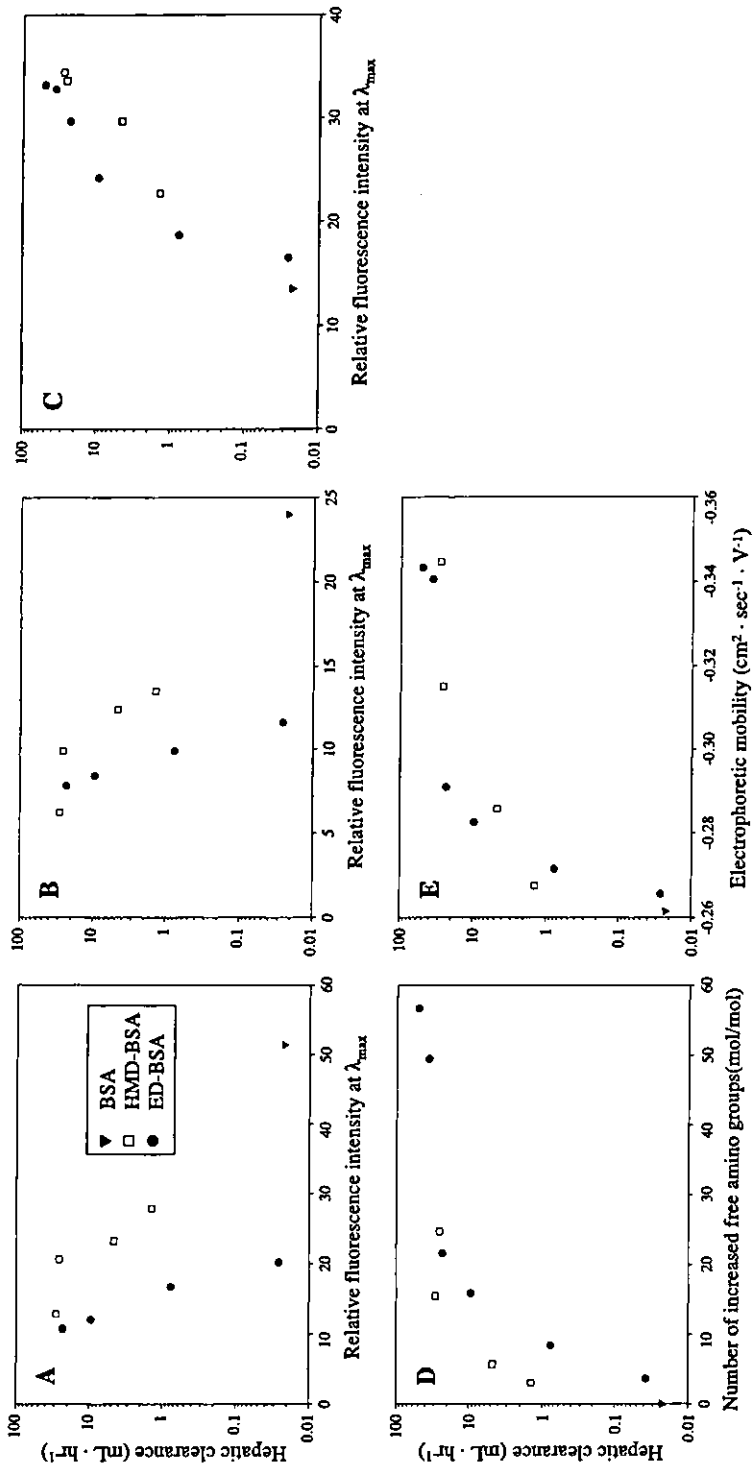

Fig. 7. Hepatic clearances of ^{111}In-labelled native and cationized BSAs as a function of the relative fluorescence intensity of native and cationized BSAs at λ_{max} excited at 280 nm (A), 295 nm (B), the effective hydrophobicity (C), the number of increased free amino groups (D) and the electrophoretic mobility (E). The data used in this figure were calculated from Table 1 and Figs. 2, 3 and 4. BSA (▼), HMD-BSA (□), ED-BSA (●).

in accessible hydrophobic areas than the ED-BSA derivatives when derivatives with a similar number of increased free amino groups were compared.

3.6. Quantitative analysis of tissue distribution characteristics of cationized BSAs

For a quantitative comparison between the distribution profiles of the native and cationized BSAs, the clearance values for the liver (CL_{liver}) were calculated based on the distribution data shown in Fig. 4. Cationization of BSA significantly increased the CL_{liver} value. The CL_{liver} of $HMD_{24.6}$-BSA (50 ml/h) was 1270-fold greater than that of BSA (0.02 ml/h). The correlation between the CL_{liver} values and the relative fluorescence intensity at λ_{max} were plotted based on the data calculated from Figs. 2 and 4. Compared with ED-BSA derivatives that have similar CL_{liver} values, the HMD-BSA derivatives remained more relative fluorescence intensity at λ_{max} both excited at 280 and 295 nm (Fig. 7A and B), indicating that there is a good correlation between the relative fluorescence intensity and the CL_{liver} values between HMD-BSA and ED-BSA. A different correlation was also observed between the effective hydrophobicity of HMD- and ED-BSA derivatives and the CL_{liver} values (Fig. 7C). In addition, when the CL_{liver} values were plotted against the increased number of free amino groups (Fig. 7D), there were considerable differences in the CL_{liver} values of HMD-BSA and ED-BSA. These differences became less significant when the CL_{liver} values were plotted against the electrophoretic mobility (μ_{ep}) (Fig. 7E), suggesting that the electrophoretic mobility is a good indicator of the hepatic uptake of amidated proteins. The CL_{liver} values increased with decreasing electrophoretic mobility towards the anode and seemed to reach a plateau at a μ_{ep} value as low as $-0.289\ cm^2 \cdot s^{-1} \cdot kV^{-1}$.

4. Discussion

Cationization is a universal approach that can be applied to increase the interaction of compounds with negatively charged biological components. Enzymes such as SOD [24], glucose oxidase [25], and catalase [25,26], as well as serum albumin [13], immunoglobulins [27] and ferritin [28], all of which are negatively charged at physiological pH, have been directly modified with diamines to obtain cationized derivatives. However, there have been few studies to examine the effect of the degree of cationization on the structural conformation and/or in vivo tissue disposition as well as the triangular relationship using different amidation reagents. Therefore, in the present study, the effect of the physicochemical properties, especially the spectroscopic and electrophoretic properties, of cationized BSA on its tissue distribution was investigated using HMD and ED as amidation modifiers.

Increasing the amounts of HMD or ED produced significant increases in the degree of modification in all cationized BSAs. There were changes in the secondary and tertiary structures of cationized BSA. Some decreases in α-helical content were also observed. The near-UV CD spectra were also modified, indicating tertiary structural changes in the environment of the disulfide bonds and aromatic amino acid residues (Fig. 1A and B) [23]. Significant changes in the intrinsic fluorescence occurred, which would result from a modification occurring in the vicinity of the Trp and Tyr residues in BSA (Fig. 2A and B) [22,23]. Furthermore, the relative fluorescence intensity at λ_{max} excited either at 280 or 295 nm decreased differently with the increasing number of free amino groups in HMD-BSA and ED-BSA (Fig. 5A and B). The effective hydrophobicity also increased in a different manner with the increasing number of free amino groups in the HMD-BSA and ED-BSA derivatives (Fig. 6). These results suggest that the extent of the spectroscopic changes in cationized BSAs depends on the increase in the number of free amino groups. This finding is in accord with the results obtained for the changes in electrophoretic properties measured by capillary electrophoresis. The cationized BSAs showed a good inverse correlation between the increased number of free amino groups and electrophoretic mobility towards the anode (Fig. 3). Briefly, the more cationic they are the more changes in their physicochemical properties occur. In addition, since the change in the μ_{ep} value is dependent on the increased number of amino groups, which is considered traditionally as an indicator of cationization, it is reasonable that the μ_{ep} value represents another new indicator of the degree of protein cationization.

Cationization of BSA greatly increased the hepatic uptake in parallel with a decrease in plasma concentration, probably due to the electrostatic interaction with anionic charges on the cell membrane surface in the liver [29]. The rate and the amount of hepatic uptake corresponded to the degree of modification. The BSA derivatives, which have a higher degree of cationization, showed a faster and more extensive hepatic uptake. To investigate the quantitative relationship between the tissue distributions of different cationized BSAs, a pharmacokinetic analysis was performed. The CL_{liver} value showed a favorable correction with the relative fluorescence intensity at λ_{max} and the effective hydrophobicity, but with different behaviors between HMD-BSA and ED-BSA (Fig. 7A, B and C). In contrast, the CL_{liver} value correlated well with the electrophoretic mobility both in HMD-BSA and ED-BSA when the μ_{ep} value was greater than $-0.289\ cm^2 \cdot s^{-1} \cdot kV^{-1}$, suggesting that an electrical charge is a critical factor for the hepatic delivery of cationized BSA (Fig. 7E). As mentioned above, the μ_{ep} value can be considered as an indicator of the degree of cationization, and this suggests that the CL_{liver} values have a good correlation with those derivatives that have a low degree of modification. On the other hand, the CL_{liver} values leveled off in those derivatives with low μ_{ep} values, which are extensively modified. As mentioned above, extensive modification would cause significant changes in the protein structure (Figs. 1-3, 5 and 6). These findings provide a useful guideline for the hepatic targeting of a protein by cationization with diamine reagent: namely derivatives with a high degree of cationization are undesirable, because extensive modification scarcely increases the hepatic uptake of cationized proteins, but does induce significant changes in their structure.

The two diamine reagents, HMD and ED, which have different numbers of CH_2 groups, were used in the present study. When HMD-BSA and ED-BSA were compared in cases where there were a similar number of increased free amino groups, slight differences were observed in the far-UV and near-UV CD spectra of these derivatives (Fig. 1A and B). However, the relative fluorescence intensity of HMD-BSA at λ_{max} changed less than that of ED-BSA (Fig. 5A and B), suggesting different behaviors of fluorescent changes occurred between HMD-BSA and ED-BSA. As shown in Fig. 6, the HMD-BSA derivatives exhibited greater hydrophobic areas than the ED-BSA derivatives. In addition, the λ_{max} value was blue-shifted only in HMD-BSA (Fig. 2A and B), indicating that more hydrophobic changes occurred around Try and/or Trp in HMD-BSAs. Because the reagents used modify the carboxyl groups of protein mainly affect the aspartic acid residue (Asp) and glutamic acid residue (Glu), HMD with a longer carboxyl side-chain could increase the hydrophobicity more than ED around the Try and/or Trp adjacent to Asp and/or Glu. Interestingly, compared with derivatives having a similar increased number of free amino groups, cationized ED-BSA showed a prolonged circulation in the blood and a slower hepatic uptake than HMD-BSA, especially at a low degree of cationization (Fig. 4). This difference was also found in the profile of the CL_{liver} values against the relative fluorescence intensity at λ_{max} (Fig. 7A and B), where different curves were obtained for HMD-BSA and ED-BSA. The HMD-BSA also showed greater CL_{liver} values than the ED-BSA when derivatives with similar numbers of increased free amino groups were compared (Fig. 7D). The difference in the number of CH_2 groups of HMD and ED, i.e., six and two CH_2 groups, respectively, would account for the difference in their structural change and tissue distribution. The interaction between the protein and the reagent, especially structural changes to the protein, such as the molecular weight, might also change in a different way after reacting with different diamine reagents. Briefly, although HMD and ED showed no significant differences as far as changing the physicochemical properties of the cationized protein was concerned, it appears that cationization reagents such as HMD, which have a longer carboxyl side-chain, have a more efficient targeting capability than ED when the increased number of free amino groups is similar.

Changes in conformation can reduce the functions of proteins. We confirmed that the conformation of BSA was changed by cationization, in a manner that depended on the reagent used and on the degree of modification. Serum albumin is responsible for a multiplicity of functions, including the maintenance of blood osmolarity, antioxidant action, properties as a solubilizing reagent and carrier for many endogenous

and exogenous compounds and a catalyst for the hydrolysis of various compounds [30,31]. In the present study, the details of the relationship between the conformational change and functional loss of cationized BSAs remain to be determined. In a preliminary study, we showed that the enzymatic action of bovine liver catalase in degrading hydrogen peroxide was reduced by cationization, to a degree which depended on the number of increased free amine groups (unpublished data). However, significant levels of activity remained after extensive conjugation of HMD or ED to catalase, suggesting the usefulness of this amidation method for targeted protein delivery.

Cationized BSAs can be rapidly taken up by the liver, suggesting that they can serve as a good carrier for liver-specific targeting of drugs the pharmacological activity of which is enhanced by targeting, such as prostaglandin E_1 [32,33]. In addition, the information obtained using cationized BSAs will be useful in developing hepatic targeting of protein drugs such as catalase.

5. Conclusion

The present study has demonstrated that electrophoretic mobility is better indicator of the degree of cationization than the increased number of free amino groups. The CL_{liver} values of cationized derivatives increase depending on the decrease in their μ_{ep} values, reaching a plateau at a high degree of cationization. The derivates with a low degree of modification are important for hepatic targeted delivery systems because the hepatic uptake of cationized BSAs correlate well with the μ_{ep} values as well as the lesser changes in the physicochemical properties.

Acknowledgements

We thank Dr. Yukihiro Kuroda of Graduate School of Pharmaceutical Sciences, Kyoto University, for his helpful advice on capillary electrophoresis.

This work was supported in part by Grants-in-Aid for Scientific Research from the Ministry of Education, Science, Sports and Culture of Japan and by 21st Century COE Program "Knowledge Information Infrastructure for Genome Science".

References

[1] H. Sezaki, M. Hashida, Macromolecular-drug conjugates in targeted cancer chemotherapy, CRC Crit. Rev. Ther. Drug Carrier Syst. 1 (1984) 1–38.
[2] H. Sezaki, Y. Takakura, M. Hashida, Soluble macromolecular carriers for the delivery of antitumor drugs, Adv. Drug Deliv. Rev. 3 (1989) 247–266.
[3] Y. Takakura, M. Hashida, Macromolecular drug carrier systems in cancer chemotherapy: macromolecular prodrugs, Crit. Rev. Oncol./Hematol. 18 (1995) 207–231.
[4] M. Hashida, Y. Takakura, Pharmacokinetics in design of polymeric drug delivery systems, J. Control. Release 31 (1994) 163–171.
[5] M. Nishikawa, Y. Takakura, M. Hashida, Pharmacokinetic evaluation of polymeric carriers, Adv. Drug Deliv. Rev. 21 (1996) 135–155.
[6] F. Staud, M. Nishikawa, Y. Takakura, M. Hashida, Liver uptake and hepato-biliary transfer of galactosylated proteins in rats are determined by the extent of galactosylatio, Biochim. Biophys. Acta 1427 (1999) 183–192.
[7] P. Opanasopit, K. Shirashi, M. Nishikawa, F. Yamashita, Y. Takakura, M. Hashida, In vivo recognition of mannosylated proteins by hepatic mannose receptors and mannan-binding protein, Am. J. Physiol.: Gasterointest. Liver Physiol. 280 (2001) G879–G889.
[8] Y. Yamasaki, K. Sumimoto, M. Nishikawa, F. Yamashita, K. Yamaoka, M. Hashida, Y. Takakura, Pharmacokinetic analysis of in vivo disposition of succinylated proteins targeted to liver nonparenchymal cells via scavenger receptors: importance of molecular size and negative charge density for in vivo recognition by receptors, J. Pharmacol. Exp. Ther. 301 (2002) 467–477.
[9] M. Hashida, R.I. Mahato, K. Kawabata, T. Miyao, M. Nishikawa, Y. Takakura, Pharmacokinetics and targeted delivery of proteins and genes, J. Control. Release 41 (1996) 91–97.
[10] Y. Yabe, M. Nishikawa, A. Tamada, Y. Takakura, M. Hashida, Targeted delivery an improved therapeutic potential of catalase by chemical modification: combination with superoxide dismutase derivatives, J. Pharmacol. Exp. Ther. 289 (1999) 1176–1184.
[11] T. Fujita, M. Nishikawa, C. Tamaki, Y. Takakura, M. Hashida, H. Sezaki, Targeted delivery of human recombinant superoxide dismutase by chemical modification with mono- and polysaccharide derivatives, J. Pharmacol. Exp. Ther. 263 (1992) 971–978.
[12] P. Opanasopit, M. Nishikawa, M. Hashida, Factors affecting drug and gene delivery: effects of interaction with blood components, Crit. Rev. Ther. Drug Carrier Syst. 19 (2002) 191–233.
[13] K. Nishida, K. Mihara, T. Takino, S. Nakane, Y. Takakura, M. Hashida, H. Sezaki, Hepatic disposition characteristics of

electrically charged macromolecules in rat in vivo and in the perfused liver, Pharm. Res. 8 (1991) 437–444.
[14] R.I. Mahato, A. Rolland, E. Tomlinson, Cationic lipid-based gene delivery systems: pharmaceutical perspectives, Pharm. Res. 14 (1997) 853–859.
[15] R.F. Chen, Removal of fatty acids from serum albumin by charcoal treatment, J. Biol. Chem. 242 (1967) 173–181.
[16] D. Triguero, J.L. Buciak, W.M. Pardridge, Cationization of immunoglobulin G results in enhanced organ uptake of the protein after intravenous administration in rats and primate, J. Pharmacol. Exp. Ther. 258 (1991) 186–192.
[17] J. Futami, T. Maeda, M. Kitazoe, E. Nukui, H. Tada, M. Seno, M. Kosaka, H. Yamada, Preparation of protein cytotoxic ribonucleases by cationization: enhanced cellular uptake and decreased interaction with ribonuclease inhibitor by chemical modification of carboxyl groups, Biochemistry 40 (2001) 7518–7524.
[18] A.F. Habeeb, Determination of free amino groups in proteins by trinitrobenzenesulfonic acid, Anal. Biochem. 14 (1966) 328–336.
[19] D.J. Hnatowich, W.W. Layne, R.L. Childs, The preparation and labeling of DTPA-coupled albumin, Int. J. Appl. Radiat. Isot. 33 (1982) 327–332.
[20] K. Yamaoka, Y. Tanigawara, T. Nakagawa, T. Uno, A pharmacokinetic analysis program (multi) for microcomputer, J. Pharmacobio-dyn. 4 (1981) 879–885.
[21] S.W. Provencher, J. Glöckneer, Estimation of globular protein secondary structure from circular dichroism, Bichemistry 20 (1981) 33–37.
[22] M. Anraku, K. Yamasaki, T. Maruyama, U. Kragh-Hansen, M. Otagiri, Effect of oxidative stress on the structure and function of human serum albumin, Pharm. Res. 18 (2001) 632–639.
[23] P.J. Coussons, J. Jacoby, A. McKay, S.M. Kelly, N.C. Price, J.V. Hunt, Glucose modification of human serum albumin: a structural study, Free Radic. Biol. Med. 22 (1997) 1217–1227.
[24] T. Takagi, M. Kitano, S. Masuda, H. Tokuda, Y. Takakura, M. Hashida, Augmented inhibitory effect of superoxide dismutase on superoxide anion release from macrophages by direct cationization, Biochim. Biophys. Acta 1335 (1997) 91–98.
[25] R. Kohen, A. Kakunda, A. Rubinstein, The role of cationizaed catalase and cationized glucose oxidase in mucosal oxidative damage induced in the rat jejunum, J. Biol. Chem. 267 (1992) 21349–21354.
[26] J. Schalkwijk, W.B. van den Berg, L.B. van de Putte, L.A. Joosten, L. van den Bersselaar, Cationization of catalase, peroxidase, and superoxide dismutase. Effect of improved intraarticular retention on experimental arthritis in mice, J. Clin. Invest. 76 (1985) 198–205.
[27] D. Triguero, J.B. Buciak, J. Yang, W.M. Pardridge, Blood–brain barrier transport of cationized immunoglobulin G: enhanced delivery compared to native protein, Proc. Natl. Acad. Sci. U. S. A. 86 (1989) 4761–4765.
[28] A.M. Dvorak, Human basophil recovery from secretion. A review emphasizing the distribution of Charcot-Leyden crystal protein in cells stained with the postfixation electron-dense tracer, cationized ferritin, Histol. Histopathol. 11 (1996) 711–728.
[29] T. Fujita, Y. Takakura, H. Sezaki, M. Hashida, Control of disposition characteristics of proteins by direct cationization in mice, Pharm. Sci. 1 (1995) 371–375.
[30] T. Peter Jr., All About Albumin, Biochemistry, Genetics, and Medical Applications, Academic Press, San Diego, 1996.
[31] Y. Sakurai, S.F. Ma, H. Watanabe, N. Yamaotsu, S. Hirono, Y. Kurono, U. Kragh-Hansen, M. Otagiri, Esterase-like activity of serum albumin: characterization of its structural chemistry using *p*-nitrophenyl esters as substrates, Pharm. Res. 21 (2004) 285–292.
[32] K. Akamatsu, Y. Yamasaki, M. Nishikawa, Y. Takakura, M. Hashida, Synthesis and pharmacological activity of a novel water-soluble hepatocyte-specific polymeric prodrug of prostaglandin E1 using lactosylated poly(L-glutamic hydrazide) as a carrier, Biochem. Pharmacol. 62 (2001) 1531–1536.
[33] K. Akamatsu, Y. Yamasaki, M. Nishikawa, Y. Takakura, M. Hashida, Development of a hepatocyte-specific prostaglandin E1 polymeric prodrug and its potential for preventing carbon tetrachloride-induced fulminant hepatitis in mice, J. Pharmacol. Exp. Ther. 290 (1999) 1242–1249.

Journal: Gt
Article : npg_gt_3302435
☐ Disk used
Pages: 1–10
Despatch Date: 2/12/2004
OP: NP/Indira

Gene Therapy (2004) 0, 1–10

www.nature.com/gt

RESEARCH ARTICLE

Hepatocyte-targeted gene transfer by combination of vascularly delivered plasmid DNA and in vivo electroporation

M Sakai[1], M Nishikawa[2], O Thanaketpaisarn[1], F Yamashita[1] and M Hashida[1]

[1]*Department of Drug Delivery Research, Graduate School of Pharmaceutical Sciences, Kyoto University, Sakyo-ku, Kyoto, Japan; and* [2]*Department of Biopharmaceutics and Drug Metabolism, Graduate School of Pharmaceutical Sciences, Kyoto University, Sakyo-ku, Kyoto, Japan*

To increase transgene expression in the liver, electric pulses were applied to the left lateral lobe after intravenous injection of naked plasmid DNA (pDNA) or pDNA/liver targeting vector complex prepared with galactosylated poly(L-lysine) or galactosylated polyethyleneimine. Electroporation (250 V/cm, 5 ms/pulse, 12 pulses, 4 Hz) after naked pDNA injection dramatically increased the expression up to 200 000-fold; the expression level obtained was significantly greater than that achieved by the combination of pDNA/vector complex and electroporation. We clearly demonstrated that the expression was dependent on the plasma concentration of pDNA at the time when the electric pulses were applied. Separation of liver cells revealed that the distribution of naked pDNA as well as transgene expression was largely selective to hepatocytes in the electroporated lobe. The number of cells expressing transgene product using vascularly administered naked pDNA followed by electroporation was significantly ($P<0.01$) greater and more widespread than that obtained by local injection of naked pDNA. These results indicate that the application of in vivo electroporation to vascularly administered naked pDNA is a useful gene transfer approach to a large number of hepatocytes.
Gene Therapy (2004) 0, 000–000. doi:10.1038/sj.gt.3302435

Keywords: *electroporation; tissue distribution; liver; hepatocytes; asialoglycoprotein receptor*

Introduction

The success of *in vivo* gene therapy relies on the development of vectors that can selectively and effectively deliver a therapeutic gene to the target with minimal toxicity. Nonviral vectors such as naked plasmid DNA (pDNA) and its complex with a cationic vector, with or without a specific ligand, has advantages over viral vectors in terms of the simplicity of use, ease of large-scale production and lack of a specific immune response.[1] However, the low efficiency of transgene expression needs to be improved. We have developed various delivery systems for pDNA, incorporating galactose[2,3] or mannose[4] to achieve cell-specific targeting to hepatocytes or liver nonparenchymal cells (NPC), respectively. These vectors were highly effective in delivering pDNA to the cells, but the transfection efficiency still needs to be improved.

A major barrier for successful *in vivo* gene transfer is the poor membrane permeability of pDNA as well as its lysosomal degradation within cells after entrance via endocytosis. Recently, various physical approaches such as electroporation,[5] sonoporation,[6] and hydrodynamic or hydrostatic pressure by large-volume injection[7,8] have been developed for improving transgene expression by nonviral vectors. Among these approaches, *in vivo* electroporation, which is suggested to transiently create pores on cell membranes[9] and has been tested in clinical trials for cancer chemotherapy,[10,11] has been extensively studied as a method to increase transgene expression by naked pDNA after local injection into the interstitial spaces of tissues. *In vivo* electroporation has been applied to various tissues including skin,[5] liver,[12,13] melanoma,[14] and muscle.[15] Generally speaking, electroporation increases transgene expression up to 1000-fold compared with that obtained with simple naked pDNA injection. However, the application of *in vivo* electroporation has been limited to locally injected pDNA, where the distribution of transgene-expressing cells is limited to a narrow area around the injection site.[16] Although the application of electric pulses to locally injected pDNA can increase the area of those cells, the spread is still limited due to the huge size of pDNA.

Vascularly administered pDNA can be distributed to a greater number of cells than locally injected pDNA. Therefore, the application of electroporation to vascularly administered pDNA could achieve transgene expression in a large target cell population. Gene therapy for the deficiency of an intracellular enzyme or structural protein requires functional restoration at the cell level, so the number of cells producing the transgene would be a major factor determining the therapeutic efficacy of the gene transfer approach. Although the application of electroporation after systemic administration of pDNA can be a promising technique to achieve this, it has

Correspondence: Dr M Nishikawa, Department of Biopharmaceutics and Drug Metabolism, Graduate School of Pharmaceutical Sciences, Kyoto University, Sakyo-ku, Kyoto 606-8501, Japan
Received 2 January 2004; accepted 4 October 2004

received little attention so far. Recently, Liu and Huang[17] published a report on electroporation-mediated gene transfer to the liver after intravenous injection of naked pDNA. They found that electroporation combined with intravenous naked pDNA can be a good method of achieving gene transfer to a larger number of liver cells compared with locally injected pDNA. However, the characteristics of gene transfer and its underlying mechanism need to be investigated to optimize this technique, in which electroporation is applied to a tissue after vascularly administered pDNA. Due to its strong negative charge, naked pDNA is rapidly taken up by the liver NPC after intravenous injection,[18,19] which results in no significant transgene expression in the organ. This uptake rapidly reduces the concentration of pDNA within the circulation. Although the results obtained by Liu and Huang[17] suggest that the distribution of pDNA would be altered by electroporation, little is known about the tissue distribution of pDNA. Targeted delivery of pDNA to hepatocytes can be achieved by galactosylated vectors, but the combined use of targeted delivery of pDNA using vectors and electroporation has not been examined so far.

We hypothesized that the application of electric pulses alters the distribution of pDNA at the site of electroporation. The liver is composed of various types of cells including hepatocytes, sinusoidal endothelial cells and Kupffer cells, and, in many genetic deficiencies such as ornithine transcarbamylase deficiency, hepatocytes can be the target of gene transfer. Therefore, we tried to achieve efficient gene transfer to hepatocytes by applying electroporation to intravenously administered pDNA. We injected pDNA into the tail vein of mice in the free form (naked pDNA) or in the complex form with a hepatocyte-targeted vector: galactosylated poly(L-lysine) (Gal-PLL)[20] or galactosylated polyethyleneimine (Gal-PEI).[3] First, the effect of electroporation was examined on the whole-body distribution of naked pDNA and pDNA/Gal-PLL using ^{32}P-labeled pDNA. Then transgene expression in the liver was evaluated after administering intravenous pDNA or its complex followed by electroporation onto the liver. As naked pDNA showed the greatest transgene expression among the vectors examined, the characteristics of the expression by naked pDNA with electroporation were investigated in detail in terms of the distribution of pDNA and transfected cells within the electroporated lobe. We report here that intravenous naked pDNA injection followed by hepatic electroporation is a good way of achieving selective gene transfer to a number of hepatocytes with a higher transfection efficiency than that offered by vector-targeted gene transfer. Hepatocytes are found to be more susceptible to the effects of electroporation than other liver NPC, and the delivery of pDNA and transgene expression are selectively improved in hepatocytes by electroporation.

Results

Effect of electroporation on pharmacokinetics of pDNA and its complex

After intravenous injection, ^{32}P-pDNA is preferentially taken up by liver NPC,[18,19] whereas a large fraction of ^{32}P-pDNA/Gal-PLL is delivered to hepatocytes through asialoglycoprotein receptor-mediated endocytosis.[20] Without electroporation, both naked ^{32}P-pDNA and ^{32}P-pDNA/Gal-PLL showed similar pharmacokinetic profiles to those reported previously; ^{32}P-radioactivity quickly disappeared from the blood circulation and accumulated in the liver (Figures 1 and 2). When naked ^{32}P-pDNA was injected, the radioactivity in the liver quickly decreased with time (Figure 1), reflecting its degradation by the organ. A set of electric pulses (250 V/cm, 5 ms/pulse, 12 pulses, 4 Hz) was applied to the left lateral lobe of the liver at 30 s after intravenous injection of either naked ^{32}P-pDNA (Figure 1) or ^{32}P-pDNA/Gal-PLL (Figure 2). No significant changes in the plasma concentration and liver accumulation of ^{32}P-radioactivity were detected in either case.

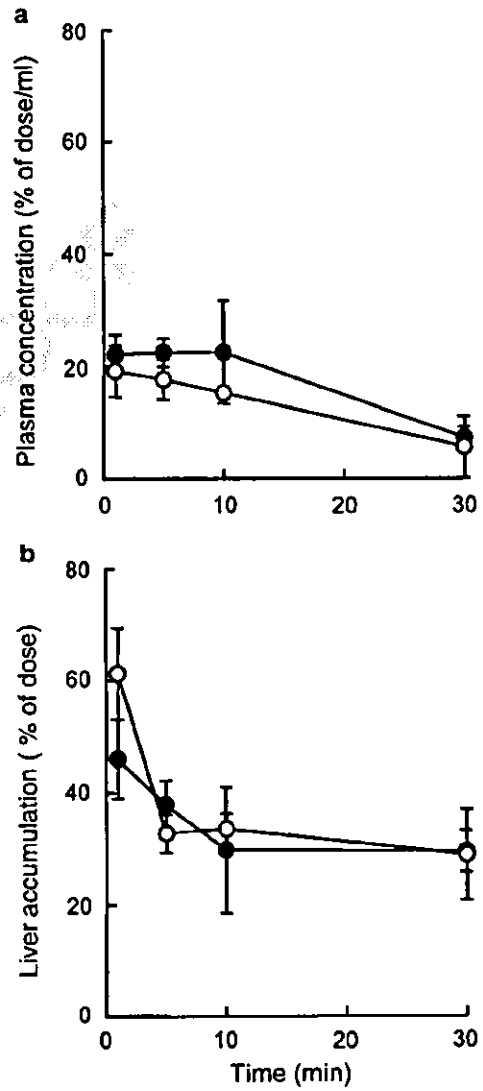

Figure 1 Plasma concentration (a) and liver accumulation (b) of ^{32}P-radioactivity after injection of naked ^{32}P-pDNA with or without electroporation. Naked ^{32}P-pDNA was injected into the tail vein at a dose of 25 μg/mouse, and electric pulses (250 V/cm, 5 ms/pulse, 12 pulses, 4 Hz) were applied to the left lateral lobe of the liver at 30 s after injection. Results are expressed as the mean ± s.d. of three mice. (○) injection only; (●) electroporated.

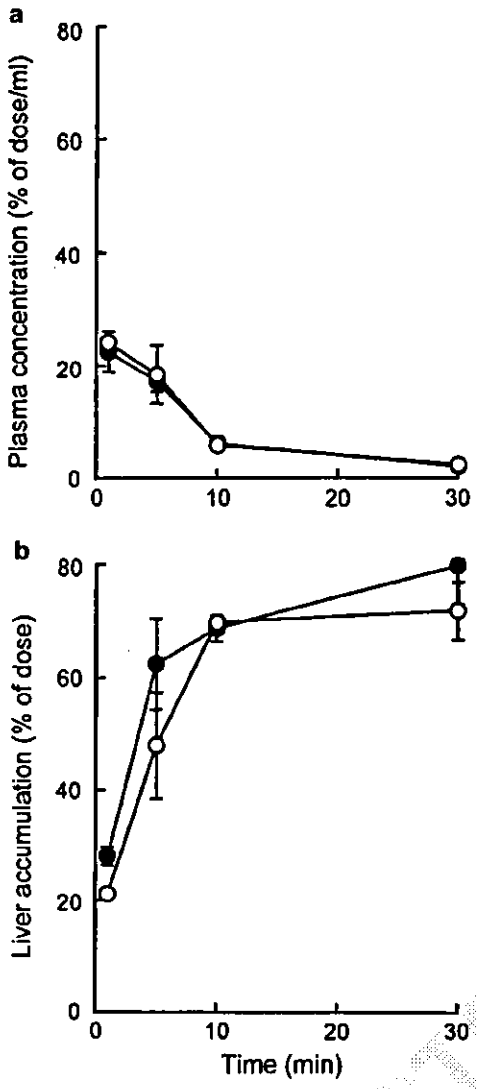

Figure 2 Plasma concentration (a) and liver accumulation (b) of ^{32}P-radioactivity after injection of ^{32}P-pDNA/Gal-PLL complex with or without electroporation. ^{32}P-pDNA/Gal-PLL complex (N/P ratio of 2.4) was injected into the tail vein at a dose of 25 μg/mouse, and electric pulses (250 V/cm, 5 ms/pulse, 12 pulses, 4 Hz) were applied to the left lateral lobe of the liver at 30 s after injection. Results are expressed as the mean ± s.d. of three mice. (○) Injection only; (●) electroporated.

Effect of electroporation on transgene expression by vascular pDNA and its complex

Transgene expression was detected at 6 h after injection of 25 μg pDNA or its complex in the following experiments. The electroporation parameters were fixed as follows unless otherwise indicated: electric field, 250 V/cm; duration of each pulse, 5 ms; number of pulses, 12; frequency of pulses, 4 Hz; timing of pulses, 30 s after injection; site of electroporation, the left lateral lobe.

No significant transgene expression was detected in the liver after intravenous injection of naked pDNA (Figure 3). pDNA/Gal-PLL or pDNA/Gal-PEI complex showed detectable transgene expression in the liver.

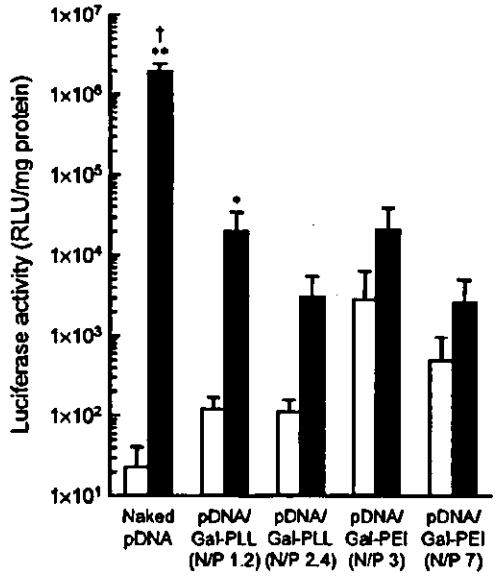

*Figure 3 Transgene expression after injection of naked pDNA, pDNA/Gal-PLL or pDNA/Gal-PEI complex with or without electroporation. pDNA complex was injected into the tail vein at a dose of 25 μg/mouse, and electric pulses (250 V/cm, 5 ms/pulse, 12 pulses, 4 Hz) were applied to the left lateral lobe of the liver at 30 s after injection. Results are expressed as the mean ± s.d. of at least three mice. (open bar) injection only; (closed bar) electroporated. *,**Statistically significant difference compared to the expression without electroporation (*P<0.01, **P<0.001). †Statistically significant difference between naked pDNA and all other groups (P<0.001).*

However, the expression level obtained was not very high, probably due to the small dose of pDNA injected. The application of electric pulses increased the expression in the electroporated lobe of the liver against any vector used (Figure 3). However, the enhancement ratio and the final level of transgene expression varied among the vectors. Naked pDNA showed the greatest enhancement ratio in transgene expression and the greatest expression level. The expression in the electroporated lobe increased up to 200 000-fold. The level of expression (about 2×10^6 RLU/mg protein) was about 100-fold greater than that obtained after the injection of pDNA complex followed by electroporation.

To confirm the effect of electroporation on the receptor-mediated gene transfer, transgene expression by naked pDNA or pDNA/Gal-PLL was examined in HepG2 cells, a human hepatoma cell line expressing asialoglycoprotein receptors. Again, electroporation increased the expression to 4500-fold for naked pDNA and nine-fold for pDNA/Gal-PLL (data not shown), suggesting that the free form of pDNA is more effective than its complexed form for transgene expression once it enters into the cytoplasm of cells.

Effect of strength of electric field on transgene expression by vascular naked pDNA

Figure 4 shows the transgene expression in the electroporated lobe and other lobes after intravenous injection of naked pDNA followed by electroporation with various electric fields from 50 to 500 V/cm. At any

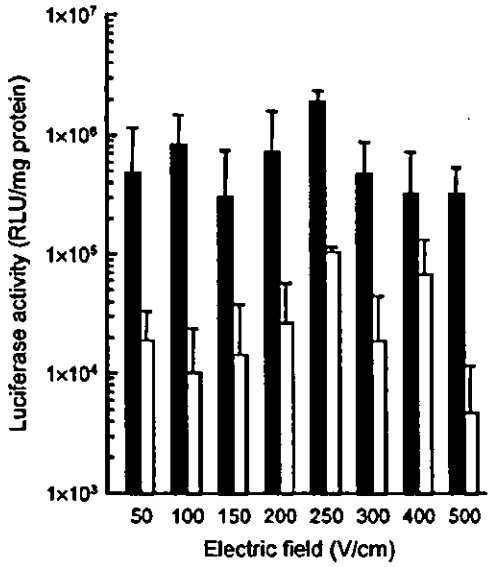

Figure 4 Effect of the strength of electric field on transgene expression after injection of naked pDNA followed by electroporation. Naked pDNA was injected into the tail vein at a dose of 25 μg/mouse, and electric pulses (50–500 V/cm, 5 ms/pulse, 12 pulses, 4 Hz) were applied to the left lateral lobe of the liver at 30 s after injection. Results are expressed as the mean ± s.d. of at least three mice. (closed bar) electroporated lobe; (open bar) nonelectroporated lobes.

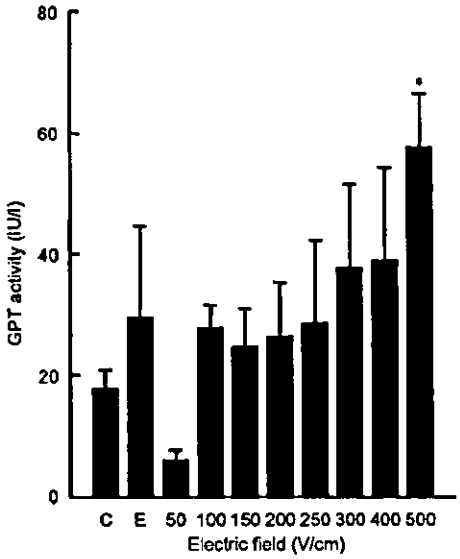

*Figure 5 GPT activity in mouse plasma after injection of naked pDNA followed by electroporation. Naked pDNA was injected into the tail vein at a dose of 25 μg/mouse, and electric pulses (50–500 V/cm, 5 ms/pulse, 12 pulses, 4 Hz) were applied to the left lateral lobe of the liver at 30 s after injection. Results are expressed as the mean ± s.d. of at least three mice. *Statistically significant difference compared to the injection only group ($P < 0.01$). C, control, electrodes were not applied to the liver; E, electrodes were applied, but pulses were not delivered.*

electric field examined, high transgene expression was obtained in the electroporated lobe, with a peak value at 250 V/cm. The expression in the nonelectroporated lobes was greater than that in the mouse liver receiving no electroporation shown in Figure 3. These results suggest that the electric pulses applied to the left lateral lobe of the liver have some influence on transgene expression in other lobes. However, there was no significant transgene expression in other organs such as the kidney, spleen, lung and heart (<100 RLU/mg protein; data not shown).

Glutamic pyruvic transferase (GPT) activity in plasma rose slightly as the electric field of the pulses increased (Figure 5). However, the activity was still low even at the highest electric field of 500 V/cm. The liver surface receiving the pulses did not show any significant changes following electroporation (data not shown).

Correlation between transgene expression and plasma concentration of pDNA

Figure 6 shows the effect of the time interval between the intravenous injection of naked pDNA and electroporation on transgene expression in the electroporated lobe. Transgene expression decreased with the interval, and became undetectable when electric pulses were applied with an interval of 20 min or longer.

Figure 7a shows the agarose gel electrophoresis of pDNA recovered from mouse plasma after intravenous injection of naked pDNA. The amounts of pDNA in supercoiled (SC), open circular (OC) and linear (L) forms were measured by densitometric analysis, and the results are summarized in Figure 7b. pDNA within the blood circulation rapidly changed its structure and decreased with time. No intact pDNA could be detected in plasma

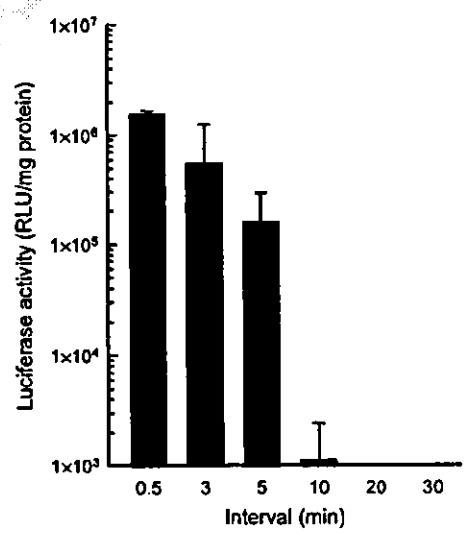

Figure 6 Effect of time interval between naked pDNA injection and electroporation on transgene expression. Naked pDNA was injected into the tail vein at a dose of 25 μg/mouse, and electric pulses (50–500 V/cm, 5 ms/pulse, 12 pulses, 4 Hz) were applied to the left lateral lobe of the liver at different intervals. Results are expressed as the mean ± s.d. of at least three mice.

at 5 min and beyond. The concentration of pDNA in plasma at electroporation correlated well with the final expression in the liver (Figure 8), suggesting that pDNA in the circulation, not captured by liver cells, is responsible for transgene expression.

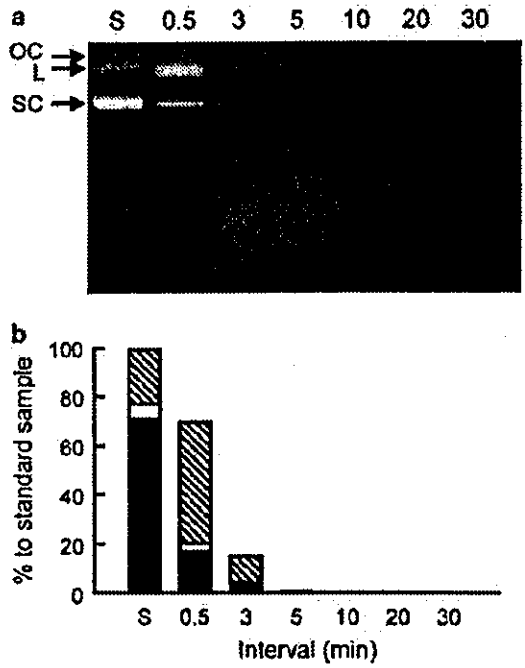

Figure 7 Stability of naked pDNA after injection into mice. (a) Naked pDNA was injected into the tail vein at a dose of 25 μg/mouse, and pDNA was recovered from mouse blood at indicated time points after injection, electrophoresed on agarose gel and visualized with ethidium bromide. (b) The amounts of pDNA in supercoiled, open circular and linear forms were measured by densitometric analysis. SC (closed bar), supercoiled; OC (open bar), open circular; L (striped bar), linear; S, standard pDNA (0.5 μg pDNA).

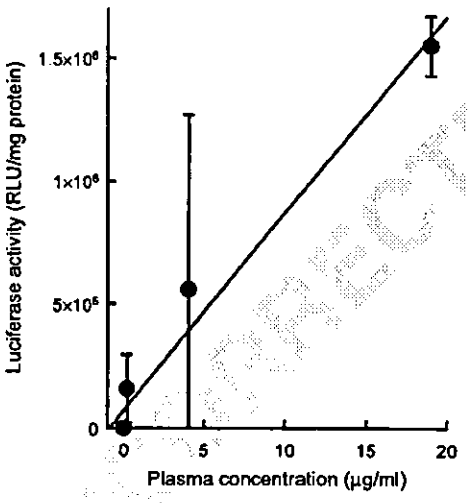

Figure 8 Relation between transgene expression and the plasma concentration of pDNA at electroporation. Transgene expression in the electroporated lobe of the liver (Figure 6) was plotted against the total concentration of pDNA (Figure 7b). Experimental details are described in the legends of Figures 6 and 7.

Cellular distribution of radioactivity and transgene expression in mouse liver after injection of naked pDNA followed by electroporation

Naked pDNA is extensively taken up by liver NPC via mechanism(s) like scavenger receptors.[18,21] In the nonelectroporated lobes of the liver, ^{32}P-radioactivity preferentially distributed to NPC rather than hepatocytes (parenchymal cells, PC) (Figure 9a). NPC uptake was about three-fold greater than PC uptake on a cell number basis, with a PC/NPC ratio of 0.35. The PC/NPC ratio increased in the electroporated lobe to 0.78, indicating that the distribution of pDNA shifted from NPC to PC by electroporation.

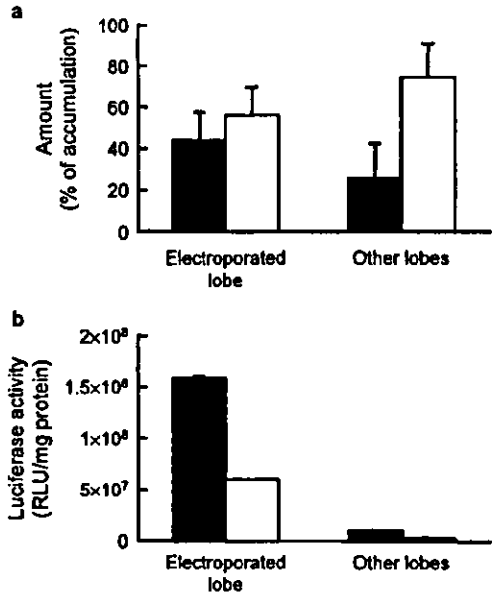

Figure 9 Distribution of ^{32}P-radioactivity (a) and luciferase activity (b) in the electroporated and nonelectroporated lobes after injection of naked pDNA followed by electroporation. Naked ^{32}P-pDNA or pDNA was injected into the tail vein at a dose of 25 μg/mouse, and electric pulses (250 V/cm, 5 ms/pulse, 12 pulses, 4 Hz) were applied to the left lateral lobe of the liver at 30 s after injection. PC (closed bar) and NPC (open bar) were separated and ^{32}P-radioactivity (a) or luciferase activity (b) in these cell fractions was assayed. Results are expressed as the mean ± s.d. of at least three mice.

As shown in Figure 4, transgene expression was very high in the electroporated lobe. Separation of the cells in the lobe clearly demonstrated that the expression in PC was significantly ($P<0.01$) greater than that in NPC (Figure 9b).

Analysis of the number of cells expressing transgene product

Figure 10b and c shows typical liver tissues receiving an intravenous injection of naked β-galactosidase-expressing pDNA followed by electroporation. For comparison, naked pDNA was directly injected into the left lateral lobe of the liver (Figure 10a), which resulted in a very localized distribution of β-galactosidase-positive cells near the injection site (arrow). Greater numbers of hepatocytes in a large area around the site of electroporation were transfected by intravenous naked pDNA followed by electroporation (Figure 10b and c).

To quantitatively evaluate the number of β-galactosidase-positive cells, we isolated hepatocytes from the left lateral lobe of the liver after administration of β-galactosidase-expressing pDNA to mice (Figure 10d).

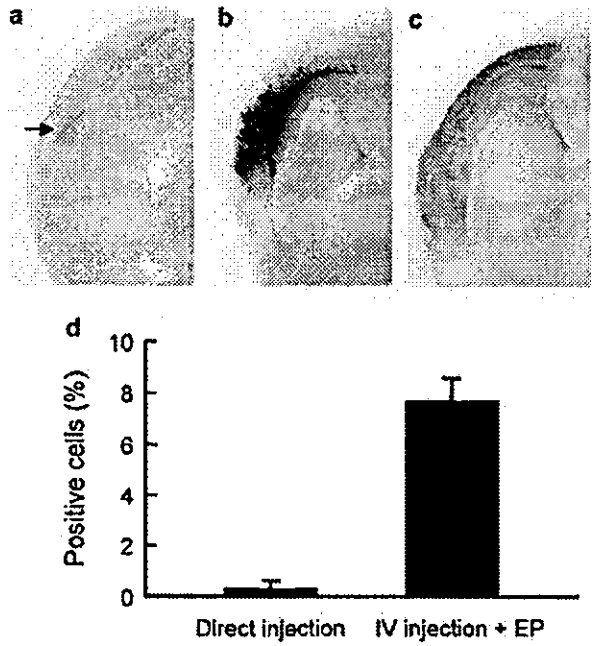

Figure 10 X-gal staining of the liver of mice receiving β-galactosidase-expressing pDNA. (a) Naked pDNA was injected directly into the left lateral lobe. (b, c) Naked pDNA was injected into the tail vein and electric pulses (250 V/cm, 5 ms/pulse, 12 pulses, 4 Hz) were applied to the left lateral lobe at 30 s after injection. (d) Hepatocytes of the left lateral lobe were isolated by collagenase perfusion and stained with X-gal as described in Materials and methods. More than 100 individual cells per sample were observed under a microscope, and the number of blue cells, that is, β-galactosidase-expressing cells, was counted. Results are expressed as the mean ± s.d. of three measurements of each sample from two mice per group.

The number of hepatocytes expressing β-galactosidase using vascularly administered naked pDNA followed by electroporation was significantly ($P < 0.01$) and about 25-fold greater than that obtained by local injection of naked pDNA.

Discussion

Naked pDNA injection is the simplest method of the nonviral gene delivery approaches. However, no significant gene expression can be detected in any tissue when naked pDNA is intravenously injected by a normal, conventional technique because of its rapid degradation and low membrane permeability. Therefore, pDNA needs to be protected from nuclease-mediated degradation by complex formation with a vector such as cationic polymer or cationic liposome.[1] Cationic vectors can increase transfection efficiency by pDNA, but the expression level seems to be still low as far as therapeutic applications are concerned. As a different challenge involving *in vivo* gene transfer, electroporation has been applied to various tissues after local injection of naked pDNA, and great improvements in transgene expression have been reported.[9] However, direct tissue injection of pDNA has the disadvantage of the limited distribution of transfected cells,[16,22,23] which would greatly restrict the efficacy of gene replacement therapy of intracellular protein.[24] These two different approaches, that is, pDNA delivery via the intravascular route and *in vivo* electroporation, could be used to achieve significant transgene expression in a large number of target cells. In a pioneer work by Liu and Huang,[17] this approach was found to be effective as far as achieving transgene expression in a greater number of liver cells was concerned. However, it was not clear how electroporation alters the distribution of pDNA within the liver. Transgene expression occurs only in the cells that take up intact pDNA into the cytoplasm. Therefore, in the present study, we focused on the changes in the distribution of pDNA and examined the option involving liver-targeted gene transfer by injecting naked or hepatocyte-targeted pDNA followed by electroporation to the organ.

As hepatocytes uniquely express asialoglycoprotein receptors on their sinusoidal surface, asialoglycoproteins or galactosylated polymers have been used to deliver a variety of pharmaceutical agents ranging from anticancer drugs to genes. Attempts to deliver pDNA to hepatocytes by conjugating or mixing it with galactose-containing vectors, however, sometimes resulted in failure because of problems in tissue distribution. We have been trying to overcome these problems by controlling the physicochemical properties of the pDNA/galactosylated vector complex.[2,3,20] In these studies, we successfully delivered pDNA to the liver, especially to hepatocytes, in amounts up to about 60% of the injected dose of pDNA. Although the pDNA complex taken up by asialoglycoprotein receptor-mediated endocytosis undergoes lysosomal degradation, a fraction is believed to be released from the endosome/lysosome pathway into the cytoplasm, then being transported into the nucleus. Some structural features have been introduced onto vectors to increase gene transfer by facilitating the release of pDNA into the cytoplasm. They are fusogenic peptides, which create pores on the plasma and/or endosomal membrane,[2,25] and polymers having buffering capacity like PEI.[26] In the present study, pDNA/galactosylated vector complexes showed greater transgene expression in the liver than naked pDNA. Of the complexes used, Gal-PEI was superior to Gal-PLL in terms of transfection efficiency to mouse liver, reflecting the buffering ability of PEI. Electroporation of a set of fixed parameters (250 V/cm, 5 ms/pulse, 12 pulses, 4 Hz) increased the expression in the electroporated lobe of the liver after intravenous injection of both pDNA/Gal-PLL and pDNA/Gal-PEI complexes. As the tissue distribution profile of ^{32}P-pDNA was hardly altered by electroporation (Figure 2), the enhanced expression would be mediated by changes in the intrahepatic and/or intracellular distribution of pDNA. Assuming that electroporation creates pores on biological membranes,[9] it is reasonable to accept that it can increase the amount of pDNA delivered to the cytoplasm prior to degradation. The pDNA/galactosylated vector complex is believed to bind to cell-surface receptors, captured in endosomes and then transported into lysosomes where it is degraded. In the present study, electric pulses were applied to a mouse at 30 s after injection of the pDNA/vector complex. However, the interval between the injection and electroporation may affect the results. The application of electric pulses at later times such as 5 or 10 min after injection did not increase the expression in the liver (data not shown). Furthermore, an increase in the amount of Gal-PLL or Gal-PEI in each complex

reduced the enhancement ratio produced by electroporation (Figure 3). These results, together with those obtained using naked pDNA, suggest that the polymers disturb to a certain degree the electroporation-mediated enhancement in transgene expression, although galactosylated vector-mediated gene transfer could be improved by *in vivo* electroporation. Different parameters involving the number, duration and electric field of electric pulses hardly improved the electroporation-mediated transgene expression by pDNA/vector complex (data not shown). The results of transgene expression in HepG2 cells strongly support the hypothesis that the free form of pDNA is more effective than its complexed form for transgene expression once it enters into the cytoplasm of cells.

In order to achieve liver-directed gene transfer, naked pDNA has been administered by various methods, including local tissue injection,[16] electroporation after local injection,[12,13] intraportal injection in a hypertonic solution,[27,28] gene gun,[29] and large-volume injection at a high velocity.[7,8] In some cases, transfection efficiency by naked pDNA exceeds that by the pDNA/vector complex. Electroporation generally increases the level of transgene expression up to 1000-fold, but the distribution of cells expressing the transgene product is still limited to around the injection site. It is expected that, when pDNA is injected into the vasculature instead of into the tissue parenchyma, it will be delivered to the vicinity of a large number of cells. Rapid injection of naked pDNA solution into the vasculature has resulted in high transgene expression in a large number of myotubes.[30] Furthermore, intraportal injection of pDNA in a hypertonic solution achieved widespread distribution of transfected cells throughout the liver.[27,28] These approaches, however, need to be studied to investigate the tissue damage induced by the procedures. Although electroporation might also induce tissue damage after its application onto the liver surface, we observed very little GPT leakage and little change in appearance, indicating that the conditions for electroporation used in this study do not result in severe tissue damage. This is marked contrast to the large volume injection of pDNA solution at high-velocity, which induced the leakage of enormous amounts of liver transaminases over a short period after injection.[31]

When intravenously injected, naked pDNA undergoes rapid degradation by nuclease and clearance by Kupffer cells, splenic macrophages, and sinusoidal endothelial cells in the liver.[18,19] No detectable transgene expression was observed in the liver. It is suggested that when electric pulses are applied to the surface of the liver, intravenously injected naked pDNA will pass through the discontinuous endothelium of the liver vascularture, reach the surface of hepatocytes, and then enter the cytoplasm through the pores created by electroporation. The application of electric pulses at different intervals clearly demonstrated that the electroporation-induced gene transfer is mediated by pDNA present in the circulation (Figure 6). There was a good correlation between the plasma concentration of undegraded pDNA and transgene expression (correlation coefficient: $r^2 = 0.97$). These findings suggest that any approach to increase the plasma retention, not to increase delivery to the liver, of pDNA could further improve electroporation-mediated gene transfer to the organ.

pDNA is significantly taken up by liver NPC due to its strong negative charge.[18,19] Electroporation did alter the distribution of ^{32}P-pDNA between hepatocytes (PC) and NPC: the distribution ratio of naked ^{32}P-pDNA to PC was greater in the electroporated lobe compared with that in the non-electroporated lobe (Figure 9a). These results suggest that electroporation selectively increases the delivery of pDNA to PC. Anatomical features do not explain the selectivity because PC are localized underneath the lining of the sinusoidal endothelial cells that should have an initial contact with vascularly injected pDNA. Canatella and Prausnitz[32] experimentally and theoretically derived an equation to predict the effects of electroporation on the uptake of solute by cells and their viability. According to this equation, the cell volume is a major factor determining the number of solute (eg pDNA) molecules delivered to the cell; liver PC, or hepatocytes, are much larger in size than liver NPC. Such a difference in size would explain the selective increase in the uptake of pDNA by hepatocytes. Transgene expression correlated well with the amount of pDNA delivered to each type of cells, and hepatocytes had a greater amount of expression than NPC. The efficiency of expression would depend on the cell type, and macrophages such as Kupffer cells undergo transfection with difficulty, which would broaden the difference between hepatocytes and other cells in terms of transgene expression.

In the present study, we successfully demonstrated that the total number of transfected cells was much greater in the liver of mice given an intravenous injection of naked pDNA followed by electroporation than in animals given a local injection of pDNA into the liver (Figure 10). A further increase in this number could be achieved by modification of the size and shape of the electrodes, because the cells between or around them were the major cells transfected.

In conclusion, a more than 200 000-fold increase in transgene expression in the liver was achieved by *in vivo* electroporation after intravenous injection of naked pDNA. pDNA in blood circulation is delivered to the inside of the cells, leading to transgene expression. Although the galactosylated vector is effective in delivering pDNA to hepatocytes through the receptor-mediated process, the vector itself can be an obstacle in the electroporation-mediated increase in transgene expression. These results indicate that the application of electroporation to vascularly administered naked pDNA is a useful gene transfer method for reaching a large number of hepatocytes, which is a key factor in determining the therapeutic efficacy of the *in vivo* gene therapy approach to treating hepatic diseases lacking any intracellular protein, liver cancer, viral hepatitis and allograft rejection. Clinical application of this approach may be achieved in combination with abdominal operation, or by the development of endoscope-type electrodes.

Materials and methods

Chemicals

[α-^{32}P]dCTP was obtained from Amersham (Tokyo, Japan). Poly(L-lysine) (PLL: average molecular weight 29 000) and branched polyethyleneimine (PEI: 70 000)

were purchased from Sigma Chemical Co. (St Louis, MO, USA) and Biowhittaker (Walkersvile, MD, USA), respectively. All other chemicals were obtained commercially as reagent-grade products. Galactosylation of PLL and PEI was performed as reported previously,[3,18] by covalently binding 2-imino-2-methoxyethyl 1-thiogalactoside to each polymer. The numbers of galactose molecules per polymer were: 44 for Gal-PLL and 60 for Gal-PEI.

Animals

Male ddY mice (5 weeks old) were purchased from Japan SLC Inc. (Shizuoka, Japan) and maintained on a standard food and water diet and housed under conventional conditions. All animal experiments were carried out in accordance with the Guidelines for Animal Experiments of Kyoto University.

Preparation of pDNA

pDNA encoding firefly luciferase cDNA under the control of CMV-IE promoter was prepared as previously reported.[2] pCMV.SPORT-βgal was purchased from GibcoBRL (GibcoBRL, Carlsbad, CA, USA). pDNA was amplified in DH5α, isolated and purified using a QIAGEN Plasmid Giga Kit (QIAGEN, Hilden, Germany). The purity of the pDNA was confirmed by 1% agarose gel electrophoresis followed by ethidium bromide staining. The pDNA concentration was measured by UV absorption at 260 nm. pDNA was labeled with [α-^{32}P]dCTP by nick translation for biodistribution experiments.[19]

Formation of pDNA complex

pDNA complex was prepared in 5% dextrose solution. Various amounts of Gal-PLL or Gal-PEI were added to pDNA, and the mixture was tapped and then left for over 30 min at room temperature. The N/P ratio, the ratio of the concentration of total nitrogen atoms in the polymer to the phosphate group (P) in pDNA, was used as an index of formation. Based on the complex formation and previous studies, N/P ratios were set at 1.2 and 2.4 for the Gal-PLL complex, and 3 and 7 for the Gal-PEI complex.

Electrodes and electric pulse delivery

Electric pulses were delivered to the liver by a pair of 1-cm^2 forceps-type electrodes connected to a rectangular direct current generator (CUY21, Nepagene, Chiba, Japan).

Electric gene delivery after systemic administration of pDNA complex

Mice were anesthetized by intraperitoneal injection of sodium pentobarbital (50 mg/kg). A midline incision was made on the abdomen and the liver was exposed. Then 5% dextrose solution of naked pDNA or pDNA complex was injected into the tail vein at a fixed dose of 25 μg pDNA/mouse. Unless otherwise indicated, electric pulses were delivered to the left lateral lobe of the liver through the electrodes at 30 s after injection. The electric pulse parameters were: 5 ms/pulse, 12 pulses, 4 Hz, and variable electric field from 50 to 500 V/cm. The incision was closed with metal clips or sutured. At 6 h after pDNA injection, the mice were killed and the liver was excised and divided into two parts: the electroporated lobe (the left lateral lobe) and the other lobes. The liver lobes were homogenized with a five-fold excess of lysis buffer (0.05% Triton X-100, 2 mM EDTA, 0.1 M Tris, pH 7.8). Then the homogenates were subjected to three cycles of freezing and thawing, and centrifuged at 10 000 *g* for 8 min at 4°C. The supernatant was used for the measurement of luciferase assay. The protein content of each supernatant was also determined using a Protein Quantification Kit (Dojindo Molecular Technologies, Kumamoto, Japan). The GPT level in plasma was measured using a GPT-UV test kit (Wako, Osaka, Japan).

In vivo distribution experiment

^{32}P-pDNA was added to unlabeled pDNA to give an injection dose of 25 μg pDNA/mouse. Each mouse was injected with ^{32}P-pDNA or its complex in 5% dextrose solution. Then, electric pulses of 250 V/cm, 5 ms/pulse, 12 pulses, 4 Hz were applied to the left lateral lobe of the liver at 30 s after injection. At 1, 5, 10 and 30 min after injection, groups of three mice each were anesthetized with ether and blood was collected from the vena cava and plasma samples were obtained by centrifugation. The liver, kidney, spleen, lung and heart were excised, rinsed with saline and weighed. These organs were homogenized with 0.05% Triton X-100 solution. Each sample was dissolved in Soluene-350 (Packard, Netherlands), then scintillation medium (Clear-sol I, Nacalai Tesque, Kyoto, Japan) was added and the ^{32}P-radioactivity was counted in an LSC-5000 liquid scintillation counter (Beckman, Tokyo, Japan). Radioactivity derived from the plasma in each tissue was corrected for as previously reported.[2]

Isolation of liver PC and NPC

pDNA or ^{32}P-pDNA was injected and electric pulses were applied as above. At 10 min (for radioactivity measurement) or 6 h (for luciferase assay) after injection, liver cells were separated into hepatocytes (PC) and NPC as reported previously.[18] In brief, the liver was perfused with a buffer containing collagenase. The dispersed cells were separated into PC and NPC fractions by differential centrifugation. These cell fractions were subjected to ^{32}P-radioactivity measurement or luciferase assay.

Stability of pDNA in plasma after intravenous injection

Mice received 25 μg pDNA into the tail vein. At indicated time points, 500 μl blood was collected from the vena cava. pDNA was extracted and electrophoresed as reported previously.[19] The amount of pDNA was evaluated by computerized densitometry.

Assessment of transgene-positive cells by X-gal staining of whole liver

Naked pCMV.SPORT-βgal (25 μg/mouse) was administered as described above. The liver was removed at 24 h after injection, then placed in a fixing solution (4% paraformaldehyde, 0.1 M NaH_2PO_4/Na_2HPO_4, pH 7.3, 2 mM $MgCl_2$, 0.01% sodium deoxycholate, and 0.02% IGEPAL C-630 (Sigma)) for 60 min at 4°C, and rinsed three times with a wash buffer (0.1 M NaH_2PO_4/Na_2HPO_4, pH 7.3, 2 mM $MgCl_2$, 0.01% sodium deoxycholate, and 0.02% IGEPAL C-630). β-Galactosidase activity was detected by immersing the liver in 5-bromo-